JOC The Journal of Organic Chemistry

Article

pubs.acs.org/joc

Internal and External Stereoisomers of Squaraine Rotaxane Endoperoxide: Synthesis, Chemical Differences, and Structural Revision

Carleton G. Collins,[†] Joshua M. Lee,[†] Allen G. Oliver,[†] Olaf Wiest,[†,‡] and Bradley D. Smith*[,†]

[†]Department of Chemistry and Biochemistry, 236 Nieuwland Science Hall, University of Notre Dame, Notre Dame, Indiana 46556, United States

[‡]Lab of Computational Chemistry and Drug Design, Laboratory of Chemical Genomics, Peking University Shenzhen Graduate School, Shenzhen 518055, P.R. China

Supporting Information

ABSTRACT: Photooxygenation of permanently interlocked squaraine rotaxanes with anthracene-containing macrocycles produces the corresponding squaraine rotaxane endoperoxides (SREPs) quantitatively. SREPs are stored at low temperature, and upon warming, they undergo clean cycloreversion, releasing singlet oxygen and emitting light. The structural elucidation in 2010 assigned the structure as the **SREP-int** stereoisomer, with the endoperoxide unit directed inside the macrocycle cavity. New experimental and computational evidence reported here proves that the initial, kinetic photooxygenation product is the less stable **SREP-ext** stereoisomer with the endoperoxide unit directed outside the macrocycle. The photophysical properties and subsequent reactivity of mechanically strained **SREP-ext** depend on the size of the end groups of the encapsulated squaraine dye. If the end groups are sufficiently large to prevent dissociation of the interlocked components, the strained **SREP-ext** stereoisomer undergoes clean thermal cycloreversion. However, smaller squaraine end groups allow transient dissociation, resulting in a pseudorotaxane dissociation/association process that produces **SREP-int** as the thermodynamic stereoisomer that does not cyclorevert. The large difference in endoperoxide reactivity for the two SREP stereoisomers illustrates the power of the mechanical bond to induce cross-component steric strain and selective enhancement of a specific reaction pathway. The new insight enabled synthetic development of triptycene-containing squaraine rotaxanes with high fluorescence quantum yields and large Stokes shifts.

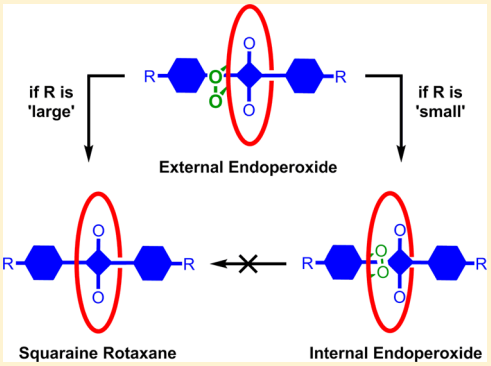

INTRODUCTION

In 2010, we reported that red light irradiation of an anthracene-containing squaraine rotaxane (**SR**) in aerated organic solution led to quantitative formation of a squaraine rotaxane endoperoxide (SREP) (Scheme 1).[1] SREPs can be stored indefinitely at temperatures below −20 °C, but upon warming to body temperature they undergo a chemiluminescent endoperoxide cycloreversion reaction that regenerates the parent **SR**. Furthermore, the color of the emitted light can be controlled over the range of green to near-infrared by simply changing the structure of the encapsulated squaraine dye.[2] Mechanistic studies have shown that the thermal cycloreversion process releases molecular oxygen, primarily in its singlet excited state, and the light emission appears to be mediated by energy transfer to the encapsulated squaraine dye.[2] The unique combination of near-infrared fluorescence and chemiluminescence makes SREPs especially attractive as storable dyes for optical imaging applications in living subjects.[3,4] An ongoing research goal is to enhance the chemiluminescence intensity, and we have investigated different strategies to increase rotaxane mechanical bond strain and accelerate the rate of cycloreversion.[5−7] In this paper, experimental and computational results are presented that necessitate a revision of our initial assignment of SREP stereochemistry and greatly expand our understanding of the structural factors that control SREP reactivity.

The limited structural data in 2010 led us to conclude that the endoperoxide unit common to all SREPs was directed inside the surrounding macrocycle (i.e., the **SREP-int** stereoisomer in Scheme 1a).[8] But new evidence reported here demonstrates that the initial kinetic product formed by oxygen cycloaddition to **SR** is the less stable **SREP-ext** stereoisomer. The photophysical properties and subsequent reactivity of the mechanically strained **SREP-ext** depend on the size of the end groups attached to the encapsulated squaraine dye. If the end groups are large enough to prevent dissociation of the interlocked components, the strained **SREP-ext** stereoisomer undergoes the thermal chemiluminescent cycloreversion reaction in Scheme 1b. However, if the squaraine end groups

Received: November 19, 2013
Published: January 15, 2014

Scheme 1

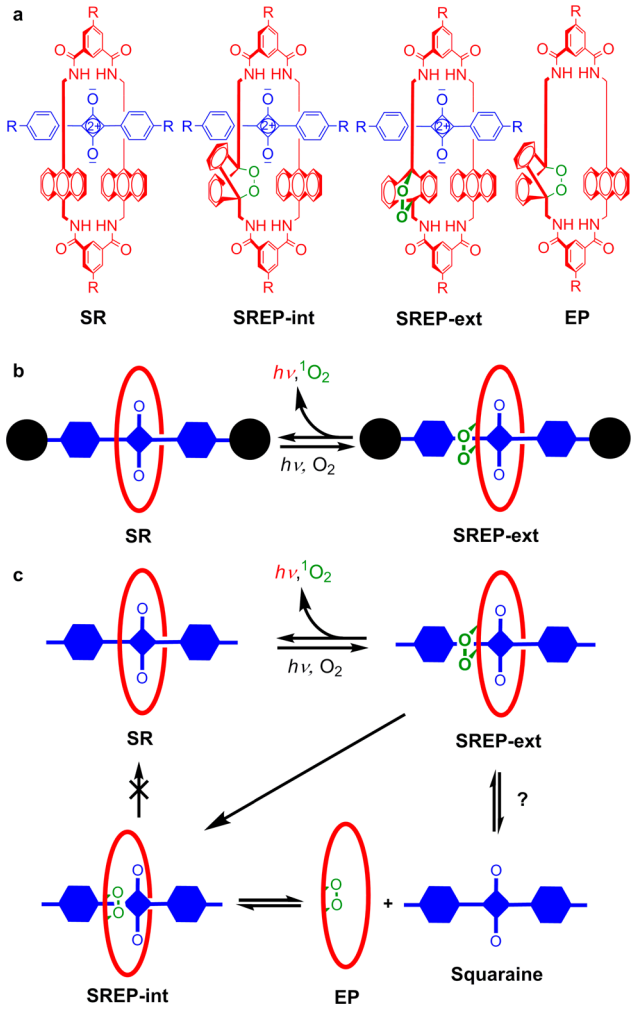

are small enough to allow transient dissociation, the result is a pseudorotaxane dissociation/association process that produces **SREP-int** as a thermodynamically more stable stereoisomer that does not undergo cycloreversion and does not emit light (Scheme 1c). The insight provided by this discovery has permitted us to develop new synthetic chemistry that adds benzyne to the exterior surface of the surrounding anthracene-containing macrocycle in **SR** to produce new squaraine rotaxane architectures with triptycene-containing macrocycles and enhanced fluorescence emission properties.

■ RESULTS AND DISCUSSION

Isolation and Structure of Macrocycle Endoperoxide 1EP. The surrounding macrocycle in a generic SREP is the tetralactam monoendoperoxide **EP**. To assess the effect of mechanical bond strain on **EP** reactivity, the free monoendoperoxide macrocycle **1EP** was prepared and its properties were characterized. We have previously reported that exposure of the parent tetralactam macrocycle **1** to singlet oxygen rapidly produces the corresponding bis(anthracene-9,10-endoperoxide) adduct with no measurable accumulation of monoendoperoxide **1EP**.[9] Thus, in order to isolate **1EP**, a stepwise templation process was developed that first produced a SREP by photooxygenation and then removed the internal squaraine dye.[10] After some experimentation, it was determined that squaraine dye **2** serves as an excellent recyclable template for the production of **1EP**. The structure of squaraine **2** is endowed with several important features that facilitate the cyclic synthetic sequence in Scheme 2. The two internal, H-

Scheme 2. Recyclable Templated Synthesis of Monoendoperoxide Macrocycle 1EP

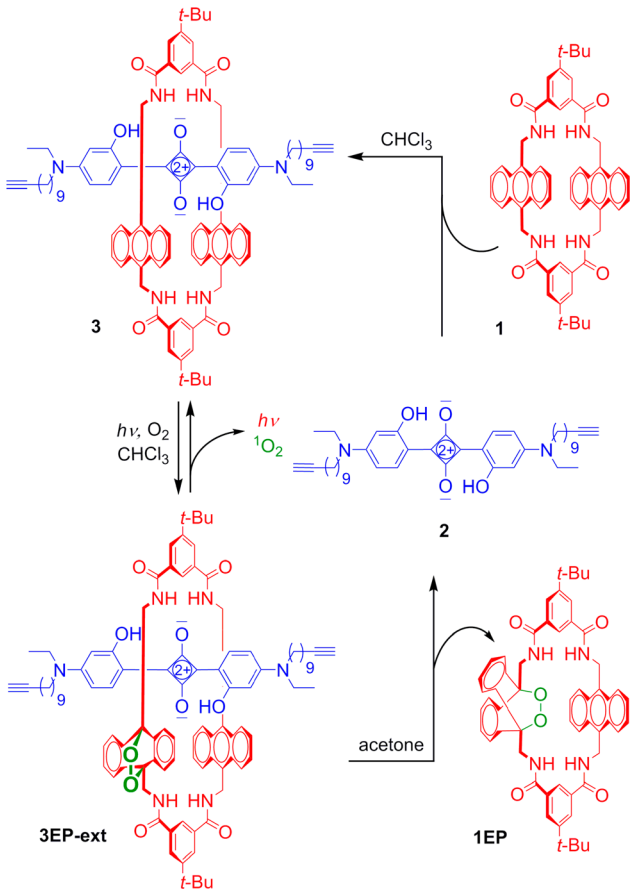

bonding hydroxyl groups on the squaraine core improve dye stability and also reduce dye affinity for the macrocyclic cavity.[11] In addition, the *N*-ethyl-*N*-nonylacetylene groups at each end of squaraine **2** are large enough to effectively block dissociation of the monoendoperoxide pseudorotaxane product, **3EP-ext** (structure elucidation of **3EP-ext** is described below), that is formed quantitatively by irradiating **3** in aerated chloroform solution.[12] Previous studies have shown that squaraine pseudorotaxane association constant is greatly reduced in polar aprotic organic solvents such as acetone.[11] Thus, forming **3EP-ext** in chloroform and then dissolving it in acetone at 5 °C leads to slow but quantitative dethreading over a 12 h period and subsequent isolation of both components (squaraine **2** and macrocycle **1EP**) in good yield using column chromatography. As expected for a 9,10-dialkylanthracene-9,10-endoperoxide, the empty macrocycle **1EP** does not undergo cycloreversion at room temperature but instead slowly decomposes through rearrangement pathways upon standing for a long time ($t_{1/2}$ ~ 10 days at 22 °C).[13] Variable-temperature ^{1}H NMR studies of pure **1EP** show no peak splitting down to −80 °C.

A sample of pure macrocycle **1EP** was crystallized from a mixed organic solvent system that included THF. The X-ray crystal structure in Figure 1 shows the endoperoxide group directed into the macrocycle cavity, which also contains a THF

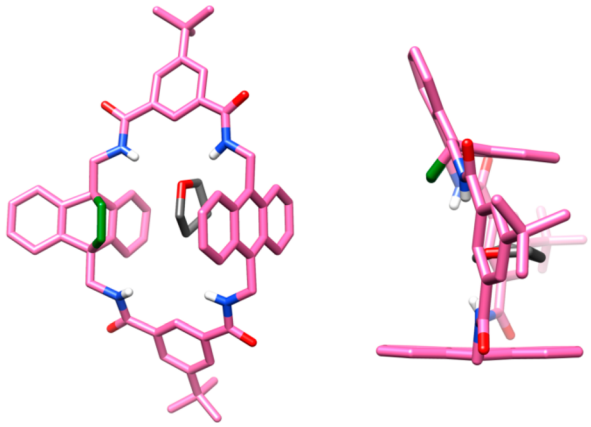

Figure 1. Side and top views of the X-ray structure of **1EP**·THF with the endoperoxide oxygen atoms colored green for clarity.

molecule that is held by bifurcated hydrogen bonds with two amide NH residues. The structure is consistent with the molecular modeling results described below, indicating that the internal endoperoxide conformation of **1EP** (**1EP-int**) is more stable than the alternative external endoperoxide conformation (**1EP-ext**). The same internal endoperoxide stereochemistry was found in the X-ray crystal structure of a closely related bis(anthracene-9,10-endoperoxide) adduct.[9]

Discovery of SREP-int and SREP-ext Stereoisomers. Since our initial report in 2010,[1] we have confirmed repeatedly that photooxygenation of permanently interlocked versions of the **SR** structure with very large squaraine end groups produces the corresponding SREP quantitatively. Moreover, the subsequent thermal cycloreversion cleanly releases molecular oxygen (mostly in the singlet excited state) and emits light.[7] Studies of various homologues show that this reversible oxygen capture and release cycle occurs equally well with rotaxane structures that encapsulate symmetric or unsymmetric squaraine dyes[1−6]

An important point with most of the **SR** structures in this study is the relatively small size of at least one of the two squaraine end groups (with exceptions discussed later). This enabled pseudorotaxane formation by mixing millimolar concentrations of the appropriate squaraine dye with macrocycle **1** in chloroform solution. In all cases, the yield of pseudorotaxane was essentially quantitative, which was expected since previous studies have shown that the association constant is around 2×10^5 M^{-1}.[14] As indicated in the section above, conversion of a **SR** to the corresponding **SREP-ext** constricts the surrounding macrocycle. As a result, the steric barrier for pseudorotaxane association/dissociation becomes more sensitive to the size of the squaraine end groups. In particular, larger squaraine end groups slow the rates of association/dissociation. A manifestation of this squaraine end group size effect became apparent when we compared the reactivity of two closely related unsymmetric squaraine pseudorotaxanes, **4** and **5**. The structure of **4** (Figure 2) has a comparatively large cyclohexamethyleneimine group at one end of the encapsulated squaraine. As shown by the changes in ^{1}H NMR spectra, irradiation of an aerated solution of **4** (Figure 2a) with red light for about 1 h at 0 °C produced the corresponding endoperoxide **4EP-ext** (Figure 2b, the structural elucidation is described below), which subsequently underwent clean cycloreversion at 38 °C ($t_{1/2}$ = 5.2 h) to regenerate **4** (Figure 2c). Thus, the relatively large size of the cyclo-

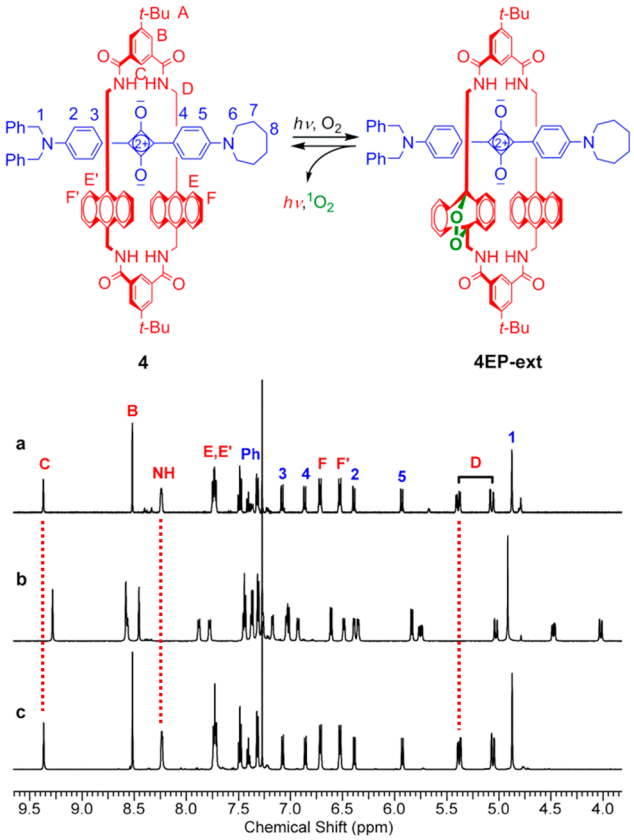

Figure 2. Chemical structures with atom assignments and ^{1}H NMR spectra in $CDCl_3$ and 22 °C showing: (a) starting sample of **4**, (b) **4EP-ext** formed by quantitative photooxygenation of **4**, (c) regenerated **4** due to cycloreversion of **4EP-ext**. The red dotted lines are provided to guide the eye.

hexamethyleneimine end group inhibits pseudorotaxane dissociation sufficiently that **4EP-ext** behaves like a permanently interlocked structure. The intercomponent mechanical bond strain selectively accelerates the endoperoxide cycloreversion reaction (Scheme 1b) so that it is preferred over the alternative endoperoxide rearrangement pathways that are typically observed with 9,10-dialkyl anthracene-9,10-endoperoxides.[13]

Shown in Figure 3 are chemical structures and NMR spectra for the analogous photooxygenation of pseudorotaxane **5** whose structure differs from **4** by only having a slightly smaller piperidine group at one end of the encapsulated squaraine. As indicated by the changes in ^{1}H NMR spectra, irradiation of **5** (Figure 3a) with red light at 0 °C cleanly produced **5EP-ext** (Figure 3b, the structural elucidation is described below). But in contrast to the behavior of **4EP-ext**, analogue **5EP-ext** subsequently underwent a spontaneous isomerization process over 3 h at 0 °C to form **5EP-int** as a thermodynamically more stable isomer (Figure 3c). Upon further standing at 38 °C, **5EP-int** did not cyclorevert back to the starting pseudorotaxane **5** but instead decomposed very slowly over several weeks (see the Supporting Information, section B). Thus, the smaller piperidine end group permitted a low barrier dissociation/association process to occur that converted the kinetic **5EP-ext** stereoisomer to the thermodynamic **5EP-int** stereoisomer. The stepwise reaction sequence in Figure 3 is a specific example of the generalized process shown in Scheme 1c and is supported by the following set of independent evidence.

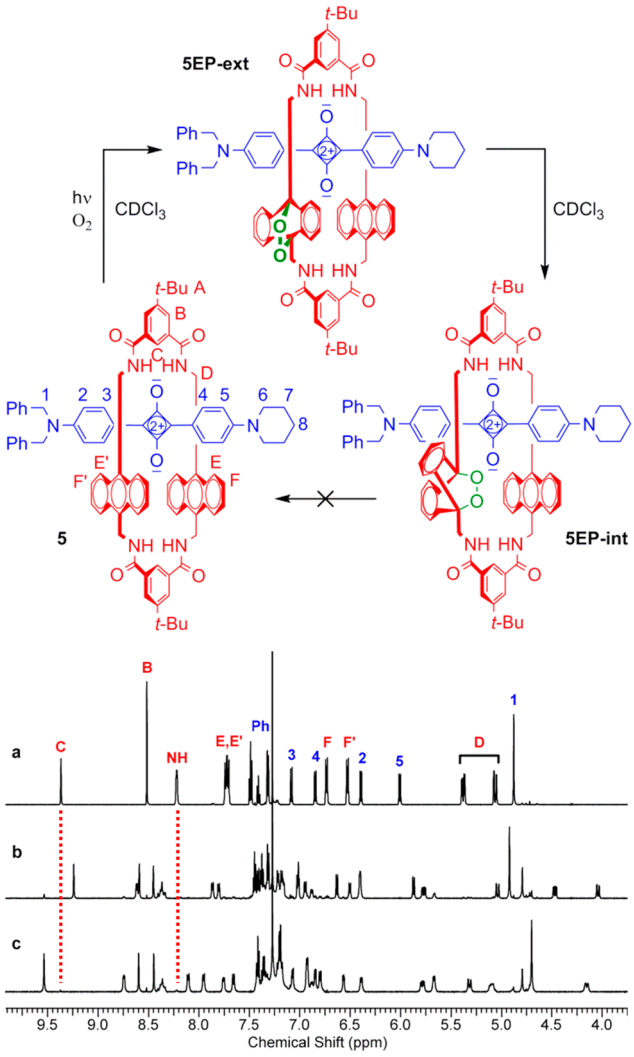

Figure 3. Chemical structures with atom assignments and ^{1}H NMR spectra of the same sample in $CDCl_3$ and 22 °C showing: (a) starting squaraine rotaxane **5**, (b) the initial kinetic product, **5EP-ext**, formed by quantitative photooxygenation of **5**, (c) the thermodynamic product **5EP-int** formed after allowing the sample of **5EP-ext** to sit for 3 h at 0 °C. The red dotted lines are provided to guide the eye.

Independent Formation of SREP-int. Strong evidence that the ^{1}H NMR spectrum in Figure 3c corresponds to **5EP-int** was gained by demonstrating that the identical NMR spectrum is produced when a sample of empty macrocycle endoperoxide **1EP** in $CDCl_3$ is mixed with 1 molar equiv of the unsymmetric squaraine dye **8**. If the thermodynamically favored isomer in Figure 3c is **5EP-int**, then it is logical to conclude that the precursor kinetically favored isomer in Figure 3b is **5EP-ext**. Furthermore, the ^{1}H NMR spectra for **5EP-ext** and **4EP-ext** (Figure 2b) are highly homologous.

Additional ^{1}H NMR experiments combined separate samples of empty macrocycle **1EP** with the different symmetric and unsymmetric squaraine dyes, **6**-**11**, shown in Scheme 3. These squaraines have at least one relatively small squaraine end group, and in each case, the corresponding pseudorotaxane (**SREP-int**) was formed in quantitative yield and did not undergo a cycloreversion reaction at 38 °C. In contrast, squaraines **12** and **13**, with slightly larger end groups, did not form a pseudorotaxane, even when mixed with 10 molar equiv of **1EP**. The extraordinary sensitivity to the size of the

Scheme 3. Squaraine Dyes That Were Tested for Inclusion Inside Empty Macrocycle Endoperoxide 1EP To Form SREP-int

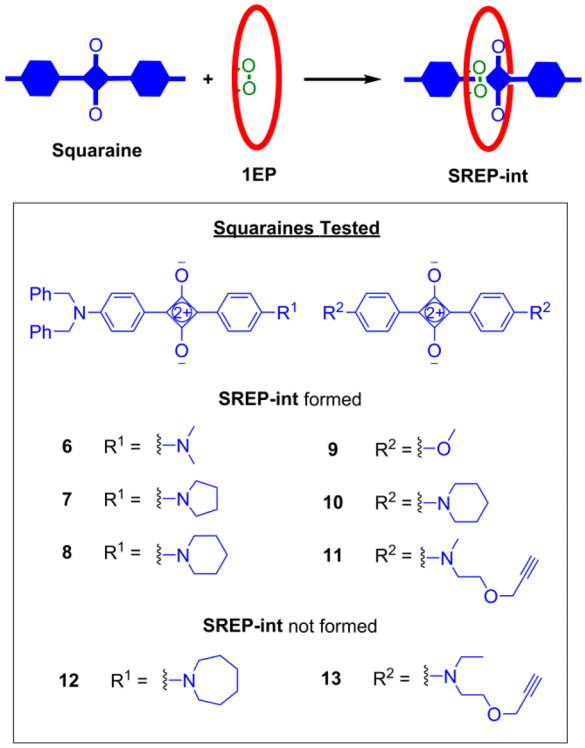

squaraine end groups is highlighted by the different outcomes obtained with squaraines **11** and **13**, where a switch from *N*-methyl to *N*-ethyl in the squaraine end groups is enough to completely block dye inclusion within the cavity of macrocycle **1EP**.[15,16]

It is worth noting that a broad comparison of ^{1}H NMR spectra for all of the different SREP compounds in this study revealed that the chemical shift of proton *C* in the bridging isophthalamide unit of the surrounding macrocycle is highly diagnostic of the SREP stereochemistry. Compared to the precursor **SR**, the signal for proton *C* is downfield in **SREP-int** and upfield in **SREP-ext** (Table 1).

Blocking Stereoisomerization by Converting a Pseudorotaxane into a Rotaxane. The pseudorotaxane dissociation/association process in Scheme 1 predicts that SREP stereoisomerization can be blocked by attaching large stopper

Table 1. Chemical Shift of Surrounding Macrocycle Proton C.[a]

encapsulated squaraine dye	SREP-ext δ (ppm)	SR δ (ppm)	SREP-int δ (ppm)
6	[b]	9.38	9.54 (0.16)
7	9.24 (−0.14)	9.37	9.54 (0.17)
8	9.24 (−0.13)	9.37	9.53 (0.16)
9	[b]	9.23	9.40 (0.17)
10	9.21 (−0.16)	9.37	9.57 (0.20)
11	9.26 (−0.12)	9.38	9.59 (0.21)
12	9.28 (−0.09)	9.37	[b]
13	9.31 (−0.08)	9.39	[b]
19	9.26 (−0.13)	9.39	9.62 (0.23)

[a]All signals were obtained at 22 °C and referenced to $CHCl_3$ at 7.27 ppm. [b]Not measured.

dx.doi.org/10.1021/jo402564k | J. Org. Chem. 2014, 79, 1120−1130

groups to the ends of the enapsulated squaraine dye. This hypothesis was confirmed by comparing separate samples of structurally related pseudorotaxane monoendoperoxide **14EP** and permanently interlocked rotaxane monoendoperoxide **15EP**. The squaraine end group in pseudorotaxane **14** includes an *N*-methyl group that is small enough to allow transient dissociation of the pseudorotaxane after conversion to the monoendoperoxide **14EP-ext**.[16] As expected, red light irradiation of an aerated $CDCl_3$ solution of pseudorotaxane **14** generated **14EP-ext** in quantitative yield (Figure 4). This

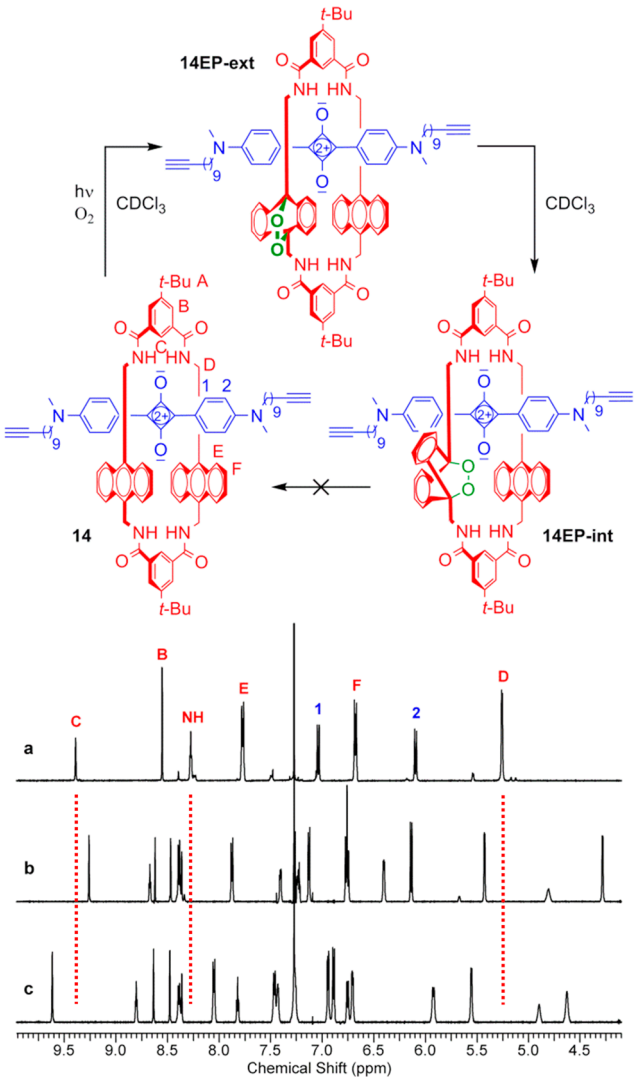

Figure 4. Chemical structures with atom assignments and ^{1}H NMR spectra of the same sample in $CDCl_3$ and 22 °C showing: (a) starting squaraine rotaxane **14**, (b) the initial kinetic product, **14EP-ext**, formed by quantitative photooxygenation of **14**, (c) the thermodynamic product **14EP-int** formed after allowing the sample of **14EP-ext** to sit for 3 h at 22 °C. The red dotted lines are provided to guide the eye.

kinetic product subsequently isomerized over 3 h at 22 °C to become the thermodynamically favored **14EP-int** which did not undergo any measurable endoperoxide cycloreversion. In contrast, red light irradiation of the permanently interlocked rotaxane **15** (prepared by clicking large stopper groups to the ends of pseudorotaxane **14**) produced the expected monoendoperoxide **15EP-ext** which did not isomerize but instead cycloreverted to the parent rotaxane **15** (Figure 5) with a half-life of 5 h at 38 °C.[17]

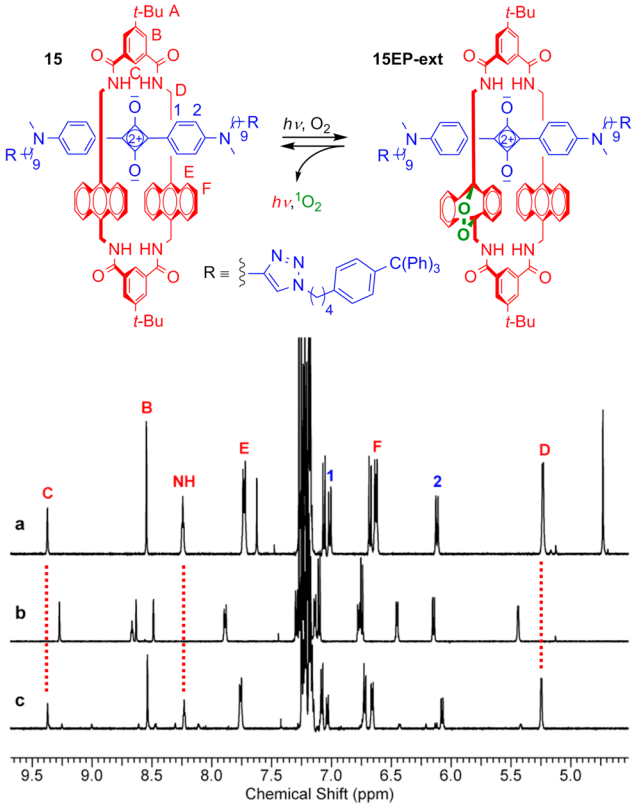

Figure 5. Chemical structures with atom assignments and ^{1}H NMR spectra in $CDCl_3$ and 22 °C showing: (a) starting sample of rotaxane **15**, (b) **15EP-ext** formed by quantitative photooxygenation of **15**, (c) regenerated **15** due to cycloreversion of **15EP-ext** over 11 h at 38 °C. The red dotted lines are provided to guide the eye.

Benzyne Cycloaddition to External Face of Anthracene Squaraine Rotaxane. The concept that dienophiles can add to the external face of the anthracene units in the **SR** structure was tested by conducting a cycloaddition reaction using the highly reactive dienophile benzyne.[18,19] Squaraine rotaxane **16** was selected because the squaraine end groups were unlikely to undergo side reactions with the excess benzyne that was generated by decomposing benzenediazonium-2-carboxylate. As summarized in Scheme 4, the benzyne cycloaddition reaction produced two major products, single addition adduct **17** in 57% isolated yield and the double addition adduct **18** in 4% isolated yield. Not only do these synthetic results strongly support the notion that dienophiles (such as singlet oxygen) can add to the exterior surface of the **SR** structure, the cycloaddition products **17** and **18** are promising new examples of triptycene-containing **SR** architectures with potentially useful spectral properties.[20] Compared to precursor **16**, the triptycene versions **17** and **18** exhibit 40% higher fluorescence quantum yields (Table 2). In addition, the Stokes shifts for **17** and **18** are >40 nm, which is unusually large for squaraines and near-infrared dyes in general.[21,22]

Molecular Modeling. A series of molecular modeling studies compared the conformations and energetics of key structures in Scheme 1. A central question is the relative stability of the two different SREP stereoisomers. Our original study included a modest set of calculations suggesting that the

Scheme 4. Cycloaddition of Benzyne and Squaraine Rotaxane 16

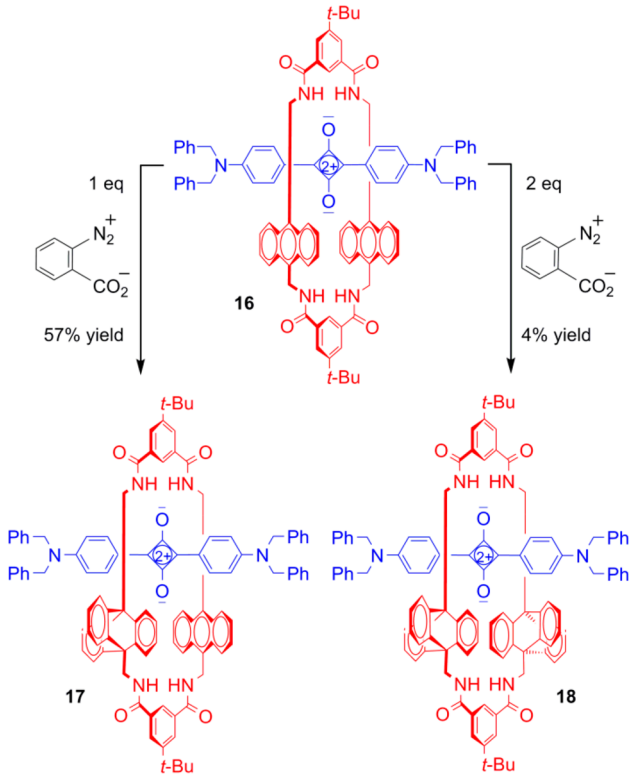

Table 2. Spectral Data

	16	17	18
λ_{abs} (nm)	657	655	652
λ_{em} (nm)	697	696	700
log ε (M^{-1} cm^{-1})	5.11[a]	5.10	4.89
Φ_f	0.48[a]	0.62[b]	0.67[b]

[a]Taken from ref 5. [b]Quantum yield measurements (±5%) were determined in $CHCl_3$ using 4,4-[bis(*N*,*N*- dimethylamino)phenyl]-squaraine dye as a reference (Φ_f = 0.70 in $CHCl_3$)[23]

SREP-int stereoisomer was more stable than **SREP-ext**.[1] A more thorough series of calculations, employing density functional theory (DFT), confirms this conclusion. Specifically, extensive DFT calculations using the model SREP system shown in Scheme 5 indicate that the lowest energy conformation of **SREP-int** is 4.0 kcal/mol more stable than the lowest energy conformation of **SREP-ext**. In other words, the kinetic product of **SR** photooxygenation, **SREP-ext**, is the less stable SREP stereoisomer, and isomerization via a pseudorotaxane dissociation/association equilibrium strongly favors **SREP-int** as the thermodynamic product. The SREP structure in our 2010 publication exhibited NMR peak splitting at −50 °C which, at the time, was attributed (incorrectly) to a macrocycle rocking motion by a putative **SREP-int** structure.[1] We have subsequently found that some SREP compounds do not exhibit any peak splitting down to −80 °C; therefore, the dynamic NMR behavior exhibited by the original SREP system is not a general phenomenon and cannot be used as a diagnostic indicator of SREP stereoisomeric structure. For a more detailed discussion of the dynamic NMR behavior of **SREP-ext**, see section D in the Supporting Information.

Scheme 5. Model SREP System Used for DFT Calculations[a]

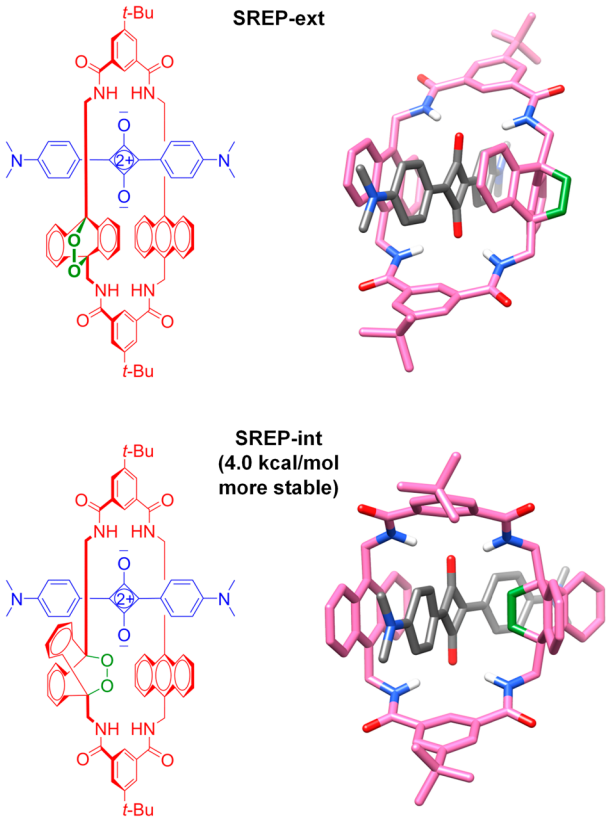

[a]The lowest energy conformation of **SREP-int** is 4.0 kcal/mol more stable than the lowest energy conformation of **SREP-ext**.

Molecular modeling of the empty endoperoxide macrocycle **1EP** determined that the lowest energy **1EP-int** conformation is 5.5 kcal/mol more stable than the alternative **1EP-ext** conformation and that conversion of **1EP-ext** to **1EP-int** occurs spontaneously at room temperature (see section I in the Supporting Information). This suggests dissociation of kinetic isomer **SREP-ext**, followed by rapid switching of the free macrocycle conformation **1EP-ext** to low energy **1EP-int**, and subsequent association to form thermodynamic isomer **SREP-int** as one possible mechanism for the SREP stereoisomerism sequence in Scheme 1c, although other variations of this theme are conceivable. For example, the **SREP-ext** dissociation step could be concerted with the macrocycle conformational switch to **1EP-int**.

We then evaluated how strain in the anthracene-9,10-endoperoxide section of macrocycle **1EP** was affected by the presence of the encapsulated squaraine dye, particularly in **SREP-ext**. Scheme 6 shows overlays of the analogous anthracene-9,10-endoperoxide moieties from *ext* and *int* conformers of **1EP** and the corresponding SREP stereoisomers. These results show that the anthracene-9,10-endoperoxide sections from **1EP-ext** and **SREP-ext** (*top*) are both noticeably flatter than the overlapped sections from **1EP-int** and **SREP-int** (*bottom*), reflecting the increased strain and deviation from ideal bond angles for the *ext* stereoisomers. The relative strain was analyzed by comparing the dihedral angle (φ) formed by the planes of the two aryl rings in the anthracene-9,10-endoperoxide moieties. In the case of the two *int* stereoisomers, the φ values of 124.1° for **SREP-int** and 120.2° for **1EP** are quite similar and correlate with a relatively unstrained

dx.doi.org/10.1021/jo402564k | J. Org. Chem. 2014, 79, 1120−1130

Scheme 6. Overlapped Pictures of the anthracene-9,10-endoperoxide Sections Excised from the Calculated Low Energy Conformations of Empty Macrocycle 1EP Conformer and Corresponding SREP Stereoisomer[a]

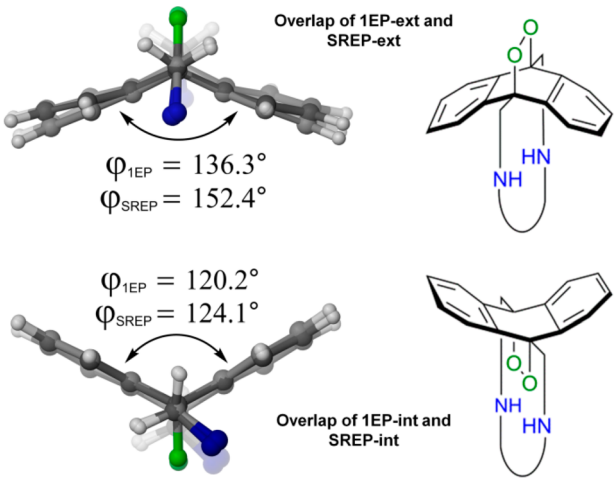

[a]In each case, the value (φ) corresponds to the dihedral angle formed by planes of the two aryl rings.

anthracene-9,10-endoperoxide system.[13,24] With the two *ext* stereoisomers, the φ value of 136.3° for **1EP** reflects moderate strain of the anthracene-9,10-endoperoxide section, and the φ value of 152.4° for **SREP-ext** indicates significantly higher strain induced by the encapsulated squaraine dye.[25] These results are consistent with the finding that the endoperoxide carbon−oxygen bonds are elongated by 0.2 Å in **SREP-ext** compared to **SREP-int**. These computational results help rationalize the experimental data. The **SREP-ext** stereoisomer undergoes a relatively facile cycloreversion reaction because the anthracene-9,10-endoperoxide is relatively strained due, in part, to cross-component steric interactions with the encapsulated squaraine dye. In contrast, the anthracene-9,10-endoperoxide in **SREP-int** stereoisomer is relatively unstrained and cycloreversion is not the lowest activation energy reaction pathway.

■ CONCLUSIONS

Photooxygenation of permanently interlocked squaraine rotaxanes (**SR**) with anthracene-containing macrocycles and very large squaraine stopper groups produces the corresponding monoendoperoxide **SREP-ext** in quantitative yield (Scheme 1). The photochemical process involves cycloaddition of photosensitized singlet-state molecular oxygen to the sterically accessible exterior surface of one of the macrocycle's anthracene units.[26,27] Although mechanically strained, samples of rotaxane **SREP-ext** can be stored indefinitely at low temperature, and upon warming to body temperature they undergo a clean thermal cycloreversion that releases singlet oxygen and emits light.[28] Structural elucidation of **SREP-ext** as the kinetic product of **SR** photooxygenation is a revision of earlier publications that incorrectly assigned the stereoisomer as **SREP-int**.[1−6] The realization that dienophiles can be added to the exterior surface of anthracene-containing squaraine rotaxanes to form the **SREP-ext** stereoisomer led us to synthesize two new squaraine rotaxane structures with triptycene-containing macrocycles (**17** and **18**) and potentially useful fluorescence emission properties.

Another notable finding of this study is that SREPs with relatively small squaraine end groups undergo spontaneous stereoisomerization from **SREP-ext** to **SREP-int**. The isomerization mechanism is a pseudorotaxane dissociation/association process that enables the initial kinetic photooxidation product, **SREP-ext**, to alleviate mechanical bond strain by converting to a thermodynamically more stable pseudorotaxane stereoisomer, **SREP-int**, that does not cyclorevert (Scheme 1c). The literature on interlocked molecules includes structural examples with functional groups forced to adopt high-energy conformations.[29] The SREP system extends this concept to functional group reactivity. The large difference in endoperoxide reactivity for the two SREP stereoisomers illustrates the power of a mechanical bond to induce cross-component steric strain and selective enhancement of a specific reaction pathway.[30]

■ EXPERIMENTAL SECTION

Compounds **1**,[14] **3**,[11] **6**,[20] **9**,[31] **13**,[14] and **16**[5] have been previously reported, and spectra of the samples used in this study are provided in the Supporting Information. The synthesis and characterization of anilines **20**, **21**, and **22** are detailed below. Anilines **23** and **24** are commercially available and were used as received. The synthesis and characterization of anilines **25**,[32] **26**,[14] and **27**[11] have been published elsewhere and are not included here. Structures of some aforementioned compounds are provided in Chart 1.

Chart 1. Synthetic Precursors

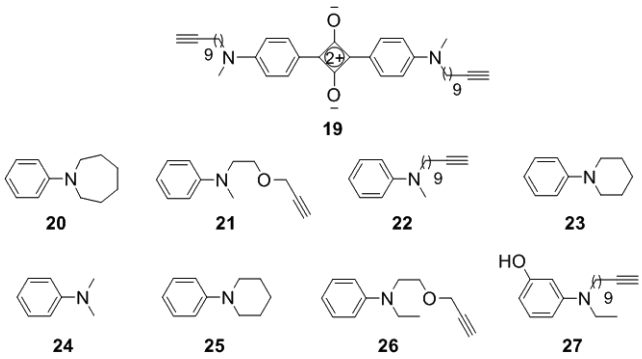

General Procedure for the Synthesis of Unsymmetrical Squaraines 7, 8, and 12. Squaraine precursor 3-(4-(dibenzylamino)-phenyl)-4-hydroxycyclobut-3-ene-1,2-dione (0.30 mmol, prepared using literature methods[13]) was dissolved in anhydrous 2-propanol (30 mL) under an atmosphere of argon. The reaction flask was charged with a solution of the appropriate aniline (0.30 mmol) in anhydrous 2-propanol (15 mL). Drying agent, tri-*n*-butyl orthoformate (1.5 mL), and anhydrous benzene (60 mL) were added, and the reaction was refluxed for 16 h with a Dean−Stark apparatus. Concentration under reduced pressure afforded crude material that was purified by silica gel column chromatography to give the desired squaraine derivative as a blue crystalline solid in the yields presented below.

Data for Squaraine **7**. A 20:80 to 30:70 (v/v) ethyl acetate/chloroform eluent was used to obtain pure **7** in 18% yield (27 mg, 0.054 mmol): mp 180−185 °C dec; ^{1}H NMR (600 MHz, $CDCl_3$) δ 8.40 (d, J = 8.8 Hz, 2H), 8.33 (d, J = 8.8 Hz, 2H), 7.35−7.38 (m, 4H), 7.29−7.32 (m, 2H), 7.20−7.21 (m, 4H), 6.85 (d, J = 9.1 Hz, 2H), 6.63 (d, J = 9.1 Hz, 2H), 4.77 (s, 4H), 3.50−3.53 (m, 4H), 2.08−2.10 (m, 4H); ^{13}C NMR (125 MHz, $CDCl_3$) δ 190.2, 187.2, 154.3, 153.2, 136.2, 134.0, 132.9, 129.0, 127.6, 126.4, 120.8, 119.8, 113.3, 112.9, 54.0, 48.3, 25.2; HRMS (ESI-TOF) calcd for $C_{34}H_{31}N_2O_2$ [M + H] 499.2380, found 499.2373.

*Data for Squaraine **8**.* A 10:90 to 20:80 (v/v) ethyl acetate/chloroform eluent was used to obtain pure **8** in 14% yield (22 mg, 0.042 mmol): mp 128−133 °C dec; ^{1}H NMR (600 MHz, $CDCl_3$) δ 8.39 (d, *J* = 9.1 Hz, 2H), 8.36 (d, *J* = 9.1 Hz, 2H), 7.35−7.39 (m, 4H), 7.29−7.33 (m, 2H), 7.20−7.22 (m, 4H), 6.89 (d, *J* = 9.7 Hz, 2H), 6.88 (d, *J* = 9.4 Hz, 2H), 4.79 (s, 4H), 3.59−3.61 (m, 4H), 1.69−1.77 (m, 6H); ^{13}C NMR (125 MHz, $CDCl_3$) δ 190.4, 188.6, 183.4, 155.3, 154.8, 136.3, 134.1, 133.3, 129.3, 127.9, 126.7, 121.1, 120.2, 113.5, 113.2, 54.2, 48.5, 26.0, 24.5; HRMS (ESI-TOF) calcd for $C_{35}H_{33}N_2O_2$ [M + H] 513.2537, found 513.2543.

*Data for Squaraine **12**.* A 10:90 (v/v) ethyl acetate/chloroform eluent was used to obtain pure **12** in (31% yield, 49 mg, 0.093 mmol): mp 172−176 °C dec; ^{1}H NMR (500 MHz, $CDCl_3$) δ 8.40 (d, *J* = 9.4 Hz, 2H), 8.35 (d, *J* = 9.2 Hz, 2H), 7.35−7.39 (m, 4H), 7.29−7.33 (m, 2H), 7.20−7.23 (m, 4H), 6.87 (d, *J* = 9.4 Hz, 2H), 6.79 (d, *J* = 9.3 Hz, 2H), 4.79 (s, 4H), 3.65 (t, *J* = 6.0 Hz, 4H), 1.82−1.88 (m, 4H), 1.58−1.62 (m, 4H); ^{13}C NMR (125 MHz, $CDCl_3$) δ 190.3, 187.3, 183.5, 155.0, 154.5, 136.4, 134.2, 133.1, 129.2, 127.9, 126.7, 121.1, 119.9, 113.1, 112.6, 54.2, 50.6, 27.3, 26.7; HRMS (ESI-TOF) calculated for $C_{36}H_{35}N_2O_2$ [M + H] 527.2693; found 527.2686.

*Data for squaraine **9**:* ^{1}H NMR (500 MHz, $CDCl_3$) δ 8.62 (d, *J* = 9.0 Hz, 4H), 7.10 (d, *J* = 9.0 Hz, 4H), 4.00 (s, 6H); ^{13}C NMR was not acquired due to the very poor solubility and stability of this squaraine; HRMS (ESI-TOF) calcd for $C_{18}H_{15}O_4$ [M + H] 295.0965, found 295.0992.

General Procedure for the Synthesis of Symmetrical Squaraines 10, 11, and 19. Squaric acid (0.30 mmol) was suspended in anhydrous *n*-butanol (30 mL), and the reaction flask was charged with a solution of the appropriate aniline (0.60 mmol) in anhydrous 2-propanol (15 mL). Anhydrous benzene (60 mL) was added, and the reaction was refluxed for 16 h with a Dean−Stark apparatus under an atmosphere of argon. Concentration under reduced pressure afforded crude material that was purified by column chromatography to give the desired squaraine derivatives as blue crystalline solids.

*Data for Squaraine **10**.* A 30:70 (v/v) ethyl acetate/chloroform eluent was used to obtain pure **10** in 13% yield (15.6 mg, 0.0389 mmol): mp 210−216 °C dec; ^{1}H NMR (600 MHz, $CDCl_3$) δ 8.38 (d, *J* = 9.1 Hz, 4H), 6.90 (d, *J* = 9.1 Hz, 4H), 3.57−3.60 (m, 8H), 1.69−1.75 (m, 12H); ^{13}C NMR (125 MHz, $CDCl_3$) δ 188.7, 183.7, 155.0, 133.6, 120.4, 113.5, 48.5, 25.9, 24.6; HRMS (ESI-TOF) calcd for $C_{26}H_{29}N_2O_2$ [M + H] 401.2224, found 401.2236.

*Data for Squaraine **11**.* A 20:70 (v/v) ethyl acetate/chloroform to a 10:90 (v/v) methanol/chloroform eluent was used to obtain pure **11** in 3.5% yield (18 mg, 0.039 mmol): mp 210−213 °C dec; ^{1}H NMR (500 MHz, $CDCl_3$) δ 8.41 (d, *J* = 9.4 Hz, 4H), 6.79 (d, *J* = 9.4 Hz, 4H), 4.17 (d, *J* = 2.4 Hz, 4H), 3.75−3.79 (m, 8H), 3.23 (s, 6H), 2.44 (t, *J* = 2.4 Hz, 2H);^{13}C NMR (125 MHz, $CDCl_3$) δ 189.5, 183.6, 154.6, 133.5, 120.3, 112.7, 79.3, 75.2, 67.5, 58.8, 52.5, 40.1; HRMS (ESI-TOF) calcd for $C_{28}H_{29}N_2O_4$ [M + H] 457.2122, found 457.2147.

*Data for Squaraine **19**.* A 10:90 to 20:80 (v/v) ethyl acetate/chloroform eluent was used to obtain pure **19** in 33% yield (86.8 mg, 0.146 mmol): mp 178−186 °C dec; ^{1}H NMR (500 MHz, $CDCl_3$) δ 8.38 (d, *J* = 9.2 Hz, 4H), 6.75 (d, *J* = 9.3 Hz, 4H), 3.48 (t, *J* = 7.6 Hz, 4H), 3.16 (s, 6H), 2.19 (td, *J* = 2.7 Hz, *J* = 7.1 Hz, 4H), 3.48 (t, *J* = 2.7 Hz, 2H), 1.63−1.69 (m, 4H), 1.53 (pent, *J* = 7.0 Hz, 4H), 1.37−1.44 (m, 4H), 1.28−1.37 (m, 16H); ^{13}C NMR (125 MHz, $CDCl_3$) 188.3, 183.7, 154.4, 133.5, 119.9, 112.4, 84.9, 68.3, 53.1, 39.1, 29.6, 29.5, 29.2, 28.9, 28.6, 27.5, 27.2, 18.6; HRMS (ESI-TOF) calcd for $C_{40}H_{53}N_2O_2$ [M + H] 593.4102, found 593.4082.

General Procedure for the Preparation of Squaraine Pseudorotaxanes. A squaraine dye (**6**−**11**) and macrocycle **1** (1 molar equiv) were dissolved in chloroform (1−5 mL) at room temperature, generating a pseudorotaxane complex quantitatively in under 5 min at 0.5−3.5 mM concentrations. All pseudorotaxane complexes were isolated as green amorphous solids.

*Data for pseudorotaxane **4**:* ^{1}H NMR (500 MHz, $CDCl_3$) δ 9.37 (t, *J* = 1.2 Hz, 2H), 8.52 (d, *J* = 1.9 Hz, 4H), 8.24 (dd, *J* = 2.8 Hz, *J* = 5.4 Hz, 4H), 7.74 (dd, *J* = 3.2 Hz, *J* = 6.8 Hz, 4H), 7.72 (dd, *J* = 3.4 Hz, *J* = 7.0 Hz, 4H), 7.47−7.51 (m, 4H), 7.38−7.42 (m, 2H), 7.30−7.33 (m, 4H), 7.08 (d, *J* = 9.2 Hz, 2H), 6.86 (d, *J* = 9.2 Hz, 2H), 6.72 (dd, *J* = 3.2 Hz, *J* = 7.0 Hz, 4H), 6.53 (dd, *J* = 3.0 Hz, *J* = 6.8 Hz, 4H), 6.39 (d, *J* = 9.4 Hz, 2H), 5.93 (d, *J* = 9.4 Hz, 2H), 5.39 (dd, *J* = 5.6 Hz, *J* = 14.8 Hz, 4H), 5.04 (dd, *J* = 2.5 Hz, *J* = 14.6 Hz, 4H), 4.88 (s, 4H), 3.56 (t, *J* = 5.6 Hz, 4H), 1.82−1.88 (m, 4H), 1.68−1.71 (m, 4H), 1.52 (s, 18H); ^{13}C NMR (125 MHz, $CDCl_3$) δ 184.1, 181.2, 178.8, 167.3, 154.3, 153.9, 153.0, 136.5, 133.5, 133.3, 133.2, 130.7, 130.6, 129.4, 129.2, 128.8, 128.3, 126.6, 126.2, 125.8, 124.4, 123.9, 122.7, 118.8, 116.5, 112.3, 111.8, 60.6, 55.2, 50.5, 35.6, 31.6, 27.6, 26.7; HRMS (ESI-TOF) calcd for $C_{92}H_{86}N_6O_6Na$ [M + Na] 1393.6501, found 1393.6526.

*Data for pseudorotaxane **5**:* ^{1}H NMR (600 MHz, $CDCl_3$) δ 9.37 (t, *J* = 1.4 Hz, 2H), 8.52 (d, *J* = 1.5 Hz, 4H), 8.22 (dd, *J* = 2.8 Hz, *J* = 5.1 Hz, 4H), 7.74 (dd, *J* = 3.2 Hz, *J* = 6.7 Hz, 4H), 7.72 (dd, *J* = 3.2 Hz, *J* = 6.7 Hz, 4H), 7.47−7.50 (m, 4H), 7.39−7.42 (m, 2H), 7.30−7.33 (m, 4H), 7.09 (d, *J* = 9.1 Hz, 2H), 6.85 (d, *J* = 9.1 Hz, 2H), 6.73 (dd, *J* = 2.9 Hz, *J* = 7.0 Hz, 4H), 6.53 (dd, *J* = 3.2 Hz, *J* = 7.0 Hz, 4H), 6.40 (d, *J* = 9.1 Hz, 2H), 6.01 (d, *J* = 9.4 Hz, 2H), 5.39 (dd, *J* = 5.6 Hz, *J* = 14.7 Hz, 4H), 5.07 (dd, *J* = 2.9 Hz, *J* = 14.9 Hz, 4H), 4.88 (s, 4H), 3.52 (t, *J* = 5.6 Hz, 4H), 1.83−1.88 (m, 2H), 1.73−1.78 (m, 4H), 1.52 (s, 18H); ^{13}C NMR (125 MHz, $CDCl_3$) δ184.1, 181.1, 179.5, 154.3, 154.1, 153.1, 136.4, 133.4, 133.2, 130.7, 130.6, 129.5, 129.2, 128.8, 128.4, 126.6, 126.2, 126.0, 124.4, 123.9, 122.7, 118.8, 116.6, 112.6, 112.3, 55.2, 48.6, 38.1, 35.6, 31.6, 26.6, 24.7; HRMS (ESI-TOF) calcd for $C_{91}H_{84}N_6O_6Na$ [M + Na] 1379.6345, found 1379.6325.

*Data for pseudorotaxane **14**:* ^{1}H NMR (500 MHz, $CDCl_3$) δ 9.39 (t, *J* = 1.4 Hz, 2H), 8.55 (d, *J* = 1.2 Hz, 4H), 8.27 (t, *J* = 4.0 Hz, 4H), 7.77 (dd, *J* = 3.4 Hz, *J* = 6.8 Hz, 8H), 7.04 (d, *J* = 9.2 Hz, 4H), 6.68 (dd, *J* = 3.2 Hz, *J* = 7.0 Hz, 8H), 6.10 (d, *J* = 9.4 Hz, 4H), 5.26 (d, *J* = 4.2 Hz, 8H), 3.47 (t, *J* = 7.6 Hz, 4H), 3.14 (s, 6H), 2.19 (td, *J* = 2.6 Hz, *J* = 7.0 Hz, 4H), 1.94 (t, *J* = 2.6 Hz, 2H), 1.71 (quint, *J* = 7.2 Hz, 4H), 1.55 (s, 18H), 1.32−1.44 (m, 24H); ^{13}C NMR (150 MHz, $CDCl_3$) δ 184.3, 179.7, 167.3, 154.0, 153.1, 133.5, 133.0, 130.7, 129.2, 128.8, 126.0, 124.2, 122.8, 117.3, 111.6, 84.9, 68.4, 53.0, 39.2, 38.2, 35.6, 31.7, 29.8, 29.7, 29.3, 28.9, 28.6, 27.8, 27.3, 18.6; HRMS (ESI-TOF) calcd for $C_{96}H_{104}N_6O_6Na$ [M + Na] 1459.7910, found 1459.7932.

General Procedures for the Preparation of Squaraine Pseudorotaxane Endoperoxides. Method A: Monoendoperoxide macrocycle **1EP** was mixed with separate samples of squaraines **6**−**11** in $CDCl_3$ at 22 °C, quantitatively generating **SREP-int** in <5 min as confirmed by ^{1}H NMR. All endoperoxide pseudorotaxane complexes were isolated as green amorphous solids. Method B: An aerated solution of squaraine pseudorotaxane **3**, **4**, **5**, or **14** (1−3 mM in $CDCl_3$) was cooled to 0 °C and irradiated with >540 nm filtered light (150 W xenon lamp) for 1.0−1.5 h to give the corresponding **SREP-ext** in quantitative yield as judged by ^{1}H NMR. The sample must be stored ≤0 °C to avoid either, cycloreversion back to the precursor squaraine pseudorotaxane in the case of **3EP-ext** or **4EP-ext**, or stereoisomerization to the more stable **SREP-int** in the case of **5EP-ext** or **14EP-ext**. All endoperoxide pseudorotaxane complexes were isolated as green amorphous solids.

*Data for pseudorotaxane endoperoxide **3EP-ext**:* ^{1}H NMR (500 MHz, $CDCl_3$) δ 10.02 (s, 2H), 9.34 (s, 2H), 8.59 (s, 2H), 8.47 (s, 2H), 8.23 (d, *J* = 6.2 Hz, 2H), 8.11 (d, *J* = 9.0 Hz, 2H), 7.61 (d, *J* = 8.8 Hz, 2H), 7.35 (d, *J* = 7.6 Hz, 2H), 7.16 (d, *J* = 4.6 Hz, 2H), 7.13 (dd, *J* = 6.6 Hz, *J* = 8.4 Hz, 2H), 6.96 (d, *J* = 7.4 Hz, 2H), 6.92 (t, *J* = 7.4 Hz, 2H), 6.79 (d, *J* = 9.4 Hz, 2H), 6.63 (dd, *J* = 6.6 Hz, *J* = 8.8 Hz, 2H), 6.22 (t, *J* = 7.4 Hz, 2H), 5.62 (d, *J* = 7.2 Hz, 2H), 5.59 (dd, *J* = 6.4 Hz, *J* = 15.4 Hz, 2H), 5.54 (s, 2H), 5.18 (d, *J* = 15.0 Hz, 2H), 4.45 (dd, *J* = 6.4 Hz, *J* = 13.8 Hz, 2H), 4.03 (dd, *J* = 1.2 Hz, *J* = 13.4 Hz, 2H), 3.43−3.53 (m, 4H), 3.33−3.43 (m, 4H), 2.20 (td, *J* = 2.6 Hz, *J* = 7.0 Hz, 4H), 1.94 (t, *J* = 2.8 Hz, 2H), 1.66−1.75 (m, 4H), 1.54 (s, 18H), 1.28−1.45 (m, 24H). ^{13}C NMR (150 MHz, $CDCl_3$, 0 °C) δ 182.4, 167.9, 167.5, 163.1, 155.8, 153.0, 135.9, 134.5, 134.0, 133.3, 133.2, 131.2, 131.1, 130.8, 130.4, 129.7, 129.3, 128.4, 126.9, 125.2, 123.8, 123.6, 122.6, 122.2, 121.3, 106.8, 100.2, 85.0, 81.6, 68.4, 51.2, 46.2, 39.3, 35.6, 32.1, 31.6, 29.9, 29.8, 29.7, 29.6, 28.9, 28.6, 27.2, 22.9, 18.6, 14.4; HRMS (ESI-TOF) calcd for $C_{98}H_{108}N_6O_{10}$ [M +] 1528.8121, found 1528.8112.

*Data for pseudorotaxane endoperoxide **4EP-ext**:* ^{1}H NMR (600 MHz, $CDCl_3$, 0 °C) δ 9.26 (s, 2H), 8.55−8.58 (m, 4H), 8.43 (s, 2H), 7.86 (dd, *J* = 3.2 Hz, *J* = 6.8 Hz, 2H), 7.76 (dd, *J* = 3.2 Hz, *J* = 7.0 Hz, 2H), 7.45 (t, *J* = 7.6 Hz, 4H), 7.38 (t, *J* = 7.3 Hz, 2H), 7.34 (d, *J* = 9.1 Hz, 2H), 7.28−7.32 (m, 6H), 7.17 (dd, *J* = 3.5 Hz, *J* = 5.0 Hz, 2H), 7.03 (dd, *J* = 3.8 Hz, *J* = 4.7 Hz, 2H), 6.98 (d, *J* = 9.1 Hz, 2H), 6.93 (dd, *J* = 2.9 Hz, *J* = 7.0 Hz, 2H), 6.60 (d, *J* = 9.1 Hz, 2H), 6.48 (dd, *J* = 2.9 Hz, *J* = 7.0 Hz, 2H), 6.39 (dd, *J* = 2.9 Hz, *J* = 5.6 Hz, 2H), 6.33 (dd, *J* = 2.9 Hz, *J* = 5.1 Hz, 2H), 5.82 (d, *J* = 9.4 Hz, 2H), 5.74 (dd, *J* = 6.8 Hz, *J* = 15.0 Hz, 2H), 5.01 (d, *J* = 15.0 Hz, 2H), 4.93 (s, 4H), 4.48 (dd, *J* = 6.7 Hz, *J* = 13.8 Hz, 2H), 4.03 (d, *J* = 13.8 Hz, 2H), 3.63−3.71 (m, 2H), 3.35−3.44 (m, 2H), 1.70−1.92 (m, 8H), 1.50 (s, 18H); ^{13}C NMR (150 MHz, $CDCl_3$, 0 °C) δ 184.2, 180.1, 176.7, 168.0, 167.8, 153.9, 153.8, 152.8, 136.3, 135.9, 135.3, 134.2, 134.1, 133.8, 133.1, 130.8, 130.6, 130.3, 130.1, 130.0, 129.8, 129.4, 128.9, 128.2, 126.4, 126.3, 124.8, 124.7, 123.7, 122.8, 122.2, 121.6, 120.4, 115.7, 112.4, 111.8, 81.2, 55.2, 50.2, 38.7, 37.0, 35.4, 31.5, 27.6, 26.7; HRMS (ESI-TOF) calcd for $C_{92}H_{87}N_6O_8$ [M + H] 1403.6580, found 1403.6587.

*Data for pseudorotaxane endoperoxide **5EP-ext**:* ^{1}H NMR (600 MHz, $CDCl_3$) δ 9.24 (s, 2H), 8.62 (d, *J* = 6.4 Hz, 2H), 8.59 (t, *J* = 1.6 Hz, 2H), 8.45 (t, *J* = 1.8 Hz, 2H), 7.87 (dd, *J* = 3.2 Hz, *J* = 6.7 Hz, 2H), 7.80 (dd, *J* = 3.2 Hz, *J* = 6.8 Hz, 2H), 7.43−7.46 (m, 4H), 7.41 (d, *J* = 9.1 Hz, 2H), 7.37 (t, *J* = 7.8 Hz, 2H), 7.30−7.32 (m, 4H), 7.21 (d, *J* = 7.3 Hz, 2H), 7.18 (dd, *J* = 3.2 Hz, *J* = 5.6 Hz, 2H), 7.16 (dd, *J* = 2.3 Hz, *J* = 6.2 Hz, 2H), 6.99−7.03 (m, 4H), 6.94 (dd, *J* = 2.9 Hz, *J* = 7.0 Hz, 2H), 6.63 (d, *J* = 9.4 Hz, 2H), 6.50 (dd, *J* = 2.9 Hz, *J* = 6.8 Hz, 2H), 6.39−6.41 (m, 4H), 5.87 (d, *J* = 9.4 Hz, 2H), 5.77 (dd, *J* = 7.1 Hz, *J* = 15.0 Hz, 2H), 5.04 (dd, *J* = 1.2 Hz, *J* = 14.6 Hz, 2H), 4.92 (s, 4H), 4.47 (dd, *J* = 6.5 Hz, *J* = 13.5 Hz, 2H), 4.04 (dd, *J* = 2.0 Hz, *J* = 13.5 Hz, 2H), 3.49 (t, *J* = 6.5 Hz, 4H), 1.82−1.86 (m, 2H), 1.74−1.78 (m. 4H), 1.51 (s, 18H).

*Data for endoperoxide pseudorotaxane **5EP-int**:* ^{1}H NMR (600 MHz, $CDCl_3$) δ 9.53 (s, 2H), 8.74 (dd, *J* = 3.5 Hz, *J* = 6.5 Hz, 2H), 8.59 (t, *J* = 1.7 Hz, 2H), 8.45 (t, *J* = 1.7 Hz, 2H), 8.10 (dd, *J* = 3.8 Hz, *J* = 8.2 Hz, 2H), 7.95 (dd, *J* = 3.8 Hz, *J* = 8.3 Hz, 2H), 7.75 (dd, *J* = 5.3 Hz, *J* = 9.4 Hz, 2H), 7.65 (d, *J* = 11.0 Hz, 2H), 7.41 (t, *J* = 7.7 Hz, 4H), 7.32−7.37 (m, 2H), 7.16−7.22 (m, 6H), 7.06 (dd, *J* = 3.2 Hz, *J* = 5.6 Hz, 2H), 6.92 (d, *J* = 7.3 Hz, 2H), 6.85 (dd, *J* = 2.9 Hz, *J* = 5.6 Hz, 2H), 6.79 (dd, *J* = 3.2 Hz, *J* = 5.6 Hz, 2H), 6.56 (dd, *J* = 2.9 Hz, *J* = 5.6 Hz, 2H), 6.38 (d, *J* = 9.7 Hz, 2H), 5.78 (dd, *J* = 7.0 Hz, *J* = 14.9 Hz, 2H), 5.67 (d, *J* = 9.1 Hz, 2H), 5.32 (d, *J* = 14.6 Hz, 2H), 5.10 (dd, *J* = 8.5 Hz, *J* = 15.2 Hz, 2H), 4.70 (s, 4H), 4.15 (d, *J* = 15.2 Hz, 2H), 3.31 (t, *J* = 5.6 Hz, 4H), 1.70−1.77 (m, 4H), 1.63−1.66 (m, 2H), 1.47 (s, 18H); ^{13}C NMR (150 MHz, $CDCl_3$) δ 186.1, 167.7, 166.4, 154.3, 154.1, 152.9, 139.6, 138.4, 136.3, 133.5, 133.3, 133.0, 132.9, 131.0, 130.8, 129.9, 129.5, 129.3, 129.2, 128.1, 127.3, 126.9, 126.8, 126.7, 126.3, 125.9, 125.0, 124.3, 122.2, 121.6, 121.3, 120.7, 112.5, 112.4, 80.6, 54.3, 48.1, 38.3, 36.9, 35.5, 31.6, 31.4, 26.3; HRMS (ESI-TOF) calcd for $C_{91}H_{84}N_6O_8K$ [M + K] 1427.5988, found 1428.5989.

*Data for endoperoxide pseudorotaxane **14EP-ext**:* ^{1}H NMR (600 MHz, $CDCl_3$) δ 9.26 (t, *J* = 1.4 Hz, 2H), 8.67 (t, *J* = 4.4 Hz, 2H), 8.62 (t, *J* = 1.6 Hz, 2H), 8.48 (t, *J* = 1.5 Hz, 2H), 7.88 (dd, *J* = 3.2 Hz, *J* = 6.7 Hz, 4H), 7.22 (t, *J* = 4.6 Hz, 2H), 7.13 (dd, *J* = 3.2 Hz, *J* = 5.4 Hz, 4H), 6.77 (dd, *J* = 3.1 Hz, *J* = 6.9 Hz, 4H), 6.43 (dd, *J* = 2.9 Hz, *J* = 5.6 Hz, 4H), 6.14 (d, *J* = 9.4 Hz, 4H), 5.43 (d, *J* = 4.1 Hz, 4H), 4.28 (d, *J* = 4.1 Hz, 4H), 3.47 (t, *J* = 7.7 Hz, 4H), 3.15 (s, 6H), 2.18 (td, *J* = 2.6 Hz, *J* = 7.3 Hz, 4H), 1.95 (t, *J* = 2.6 Hz, 2H), 1.68−1.73 (m, 4H), 1.62−1.68 (m, 4H), 1.53 (s, 18H), 1.30−1.38 (m, 20H).

*Data for endoperoxide pseudorotaxane **14EP-int**:* ^{1}H NMR (500 MHz, $CDCl_3$) δ 9.62 (t, *J* = 1.6 Hz, 2H), 8.80 (t, *J* = 5.0 Hz, 2H), 8.64 (t, *J* = 1.8 Hz, 2H), 8.48 (t, *J* = 1.7 Hz, 2H), 8.05 (dd, *J* = 3.4 Hz, *J* = 7.0 Hz, 4H), 7.82 (t, *J* = 5.8 Hz, 2H), 7.46 (d, *J* = 8.8 Hz, 4H), 6.94 (dd, *J* = 3.2 Hz, *J* = 5.6 Hz, 4H), 6.89 (dd, *J* = 3.2 Hz, *J* = 7.0 Hz, 4H), 6.71 (dd, *J* = 3.1 Hz, *J* = 5.6 Hz, 4H), 5.92 (d, *J* = 8.4 Hz, 4H), 5.56 (d, *J* = 4.4 Hz, 4H), 4.62 (br. s, 4H), 3.31 (t, *J* = 7.6 Hz, 4H), 2.99 (s, 6H), 2.19 (td, *J* = 2.6 Hz, *J* = 7.2 Hz, 4H), 1.94 (t, *J* = 2.6 Hz, 2H), 1.47−1.56 (m, 8H), 1.52 (s, 18H), 1.30−1.38 (m, 20H); HRMS (ESI-TOF) calcd for $C_{96}H_{105}N_6O_8$ [M + H] 1470.8021, found 1470.8037.

Squaraine Rotaxane 15. Pseudorotaxane **14** (9.6 mg, 6.7 μmol) was combined with 1-(4-azidobutoxy)-4-(triphenylmethyl)benzene (11.4 mg, 26.3 μmol) in chloroform (5 mL). *N,N*-Diisopropylethylamine (2 drops) and tris[(1-benzyl-1*H*-1,2,3-triazol-4-yl)methyl]-amine copper(I)bromide (2.5 mg, 3.7 μmol) were added, and the reaction was stirred at rt for 16 h. The reaction was washed with saturated aqueous EDTA solution (5 mL), and the organic layer was collected and evaporated under reduced pressure. The crude product that was purified using silica gel column chromatography, using a 20:80 to 50:50 (v/v) ethyl acetate/chloroform eluent gradient to obtain pure **15** (84% yield, 13.0 mg, 5.64 μmol) as a green amorphous solid: ^{1}H NMR (600 MHz, $CDCl_3$) δ 9.39 (t, *J* = 1.7 Hz, 2H), 8.55 (d, *J* = 0.9 Hz, 4H), 8.27 (t, *J* = 4.4 Hz, 4H), 7.77 (dd, *J* = 3.5 Hz, *J* = 7.1 Hz, 8H), 7.22−7.27 (m,16H), 7.16−7.22 (m, 16H), 7.09 (d, *J* = 8.8 Hz, 4H), 7.03 (d, *J* = 9.4 Hz, 4H), 6.74 (d, *J* = 8.8 Hz, 4H), 6.67 (dd, *J* = 3.2 Hz, *J* = 7.0 Hz, 8H), 6.09 (d, *J* = 9.4 Hz, 4H), 5.25 (d, *J* = 3.8 Hz, 8H), 4.38 (t, *J* = 7.3 Hz, 4H), 3.94 (t, *J* = 5.8 Hz, 4H), 3.46 (t, *J* = 7.9 Hz, 4H), 3.13 (s, 6H), 2.70 (t, *J* = 7.9 Hz, 4H), 2.08 (pent, *J* = 7.4 Hz, 4H), 1.77 (pent, *J* = 5.8 Hz, 4H), 1.65−1.73 (m, 4H), 1.54 (s, 18H), 1.37−1.44 (m, 20H); ^{13}C NMR (150 MHz, $CDCl_3$) δ 184.3, 179.6, 167.3, 156.8, 154.0, 153.1, 148.6, 147.2, 139.3, 133.5, 133.0, 132.4, 131.3, 130.6, 129.2, 128.8, 127.6, 126.1, 126.0, 124.2, 122.8, 120.7, 117.3, 113.3, 111.6, 66.9, 64.5, 53.0, 50.0, 39.2, 38.2, 35.6, 31.7, 29.9, 29.8, 29.7, 29.6, 29.5, 29.4, 27.8, 27.5, 27.2, 26.5, 25.9; HRMS (ESI-TOF) calcd for $C_{154}H_{159}N_{12}O_8$ [M^{2+}] 1152.1196, found 1152.1183.

Squaraine rotaxane endoperoxide 15EP-ext: ^{1}H NMR (600 MHz, $CDCl_3$) δ 9.25 (s, 2H), 8.66 (t, *J* = 4.1 Hz, 2H), 8.61 (t, *J* = 1.7 Hz, 2H), 8.47 (t, *J* = 1.7 Hz, 2H), 7.87 (dd, *J* = 3.2 Hz, *J* = 7.0 Hz, 4H), 7.22−7.28 (m,18H), 7.16−7.20 (m, 18H), 7.12 (dd, *J* = 3.2 Hz, *J* = 5.6 Hz, 4H), 7.09 (d, *J* = 8.8 Hz, 4H), 6.76 (dd, *J* = 2.9 Hz, *J* = 7.0 Hz, 4H), 6.73 (d, *J* = 9.1 Hz, 4H), 6.43 (dd, *J* = 2.9 Hz, *J* = 5.6 Hz, 4H), 6.13 (d, *J* = 9.1 Hz, 4H), 5.42 (d, *J* = 4.1 Hz, 4H), 4.37 (t, *J* = 7.0 Hz, 4H), 4.25 (d, *J* = 4.1 Hz, 4H), 3.93 (t, *J* = 5.9 Hz, 4H), 3.45 (t, *J* = 7.9 Hz, 4H), 3.13 (s, 6H), 2.68 (t, *J* = 7.6 Hz, 4H), 2.07 (pent, *J* = 7.6 Hz, 4H), 1.77 (pent, *J* = 5.9 Hz, 4H), 1.62−1.71 (m, 8H), 1.52 (s, 18H), 1.38−1.42 (m, 8H), 1.32−1.37 (m, 12H); ^{13}C NMR (150 MHz, $CDCl_3$, 0 °C) δ 184.5, 178.4, 168.1, 167.8, 156.7, 153.7, 152.8, 148.6, 147.0, 139.2, 135.7, 134.0, 133.9, 133.2, 132.2, 131.2, 130.8, 130.6, 130.2, 129.9, 129.0, 127.6, 126.0, 125.5, 124.4, 122.8, 121.9, 120.7, 117.8, 113.1, 111.6, 81.2, 66.8, 64.3, 53.0, 50.0, 39.2, 38.7, 37.1, 35.5, 31.5, 29.9, 29.7, 29.6, 29.5, 29.4, 27.8, 27.5, 27.2, 26.3, 25.8, 22.9; HRMS (ESI-TOF) calcd for $C_{154}H_{159}N_{12}O_{10}$ [M + H] 2336.2297, found 2336.2312.

Monoendoperoxide Macrocycle 1EP. Endoperoxide pseudorotaxane **3EP** (19 mg, 12 μmol) was dissolved in acetone (20 mL) and allowed to dethread over 12 h at 5 °C. The resulting blue solution was evaporated under reduced pressure and purified by silica gel column chromatography. A 10:90 (v/v) ethyl acetate/chloroform eluent was used to obtain **1EP** (91% yield, 9.7 mg, 11 μmol) as a white solid. On occasion, unoxidized macrocycle **1** contaminates the sample, which can be removed via selective templation of **1** with squaraine **13** (**1EP** does not complex **13**). The resulting pseudorotaxane can be separated from **1EP** by silica gel column chromatography using a 20:20:60 (v/v/v) ethyl acetate/hexanes/chloroform eluent to provide purified **1EP** as an amorphous white solid: ^{1}H NMR (500 MHz, $CDCl_3$) δ 8.41 (t, *J* = 2.2 Hz, 2H), 8.39 (dd, *J* = 3.4 Hz, *J* = 7.1 Hz, 4H), 8.34 (t, *J* = 1.8 Hz, 2H), 7.59 (dd, *J* = 3.2 Hz, *J* = 7.0 Hz, 4H), 7.37 (dd, *J* = 3.4 Hz, *J* = 5.6 Hz, 4H), 7.28 (t, *J* = 1.4 Hz, 2H), 7.20 (dd, *J* = 3.2 Hz, *J* = 5.6 Hz, 4H), 6.40 (t, *J* = 5.6 Hz, 2H), 6.36 (t, *J* = 4.0 Hz, 2H), 5.68 (d, *J* = 4.4 Hz, 4H), 4.81 (d, *J* = 5.8 Hz, 4H), 1.45 (s, 18H); ^{13}C NMR (150 MHz, $CDCl_3$) δ 167.2, 166.8, 153.7, 138.5, 133.8, 132.8, 130.6, 130.4, 130.0, 129.6, 128.3, 127.0, 124.9, 121.6, 119.1, 81.3, 38.6, 37.5, 31.4, 29.9; HRMS (ESI-TOF) calcd for $C_{56}H_{52}N_4O_6Na$ [M + Na] 899.3761, found 899.3779.

Procedure for the Preparation of Triptycene Squaraine Rotaxanes 17 and 18. Anthranilic acid (515 mg, 3.76 mmol) and trichloroacetic acid (10 mg, 0.061 mmol) were dissolved in anhydrous THF (20 mL) under a dry atmosphere of argon. The reaction was cooled to −5 °C, and isopentyl nitrite (0.82 mL, 0.72 g, 6.1 mmol) was added over 10 min. The mixture was stirred for 45 min at 0 °C and then allowed to warm to room temperature for 1 h (a blast shield was used during this sequence). The benzenediazonium-2-carboxylate

precipitate was collected via filtration using minimal suction and washed with cold THF, making sure not to let the filtrate go dry (Safety warning: this diazonium salt is potentially shock sensitive and may violently detonate when dry). The wet filtrate was immediately transferred to a solution of rotaxane **16** (23.3 mg, 15.9 μmol) in dichloroethane (25 mL), and the mixture was heated at 40 °C for 15 min. After the reaction mixture was cooled to room temperature, the solution was evaporated under reduced pressure and purified via silica gel column chromatography using a 10:20:70 (v/v/v) ethyl acetate/hexanes/chloroform eluent to provide a mixture of cycloadducts **17** and **18**. Rotaxanes **17** (57% yield, 14 mg, 9.0 μmol) and **18** (4% yield, 1.1 mg, 0.68 μmol) were separated using multiple preparative TLC purifications with a 10:10:80 (v/v/v) ethyl acetate/hexanes/chloroform solvent system. They were isolated as green amorphous solids.

*Data for squaraine rotaxane **17**:* ^{1}H NMR (600 MHz, $CDCl_3$) δ 9.52 (t, *J* = 1.5 Hz, 2H), 8.62 (t, *J* = 3.5 Hz, 2H), 8.57 (t, *J* = 1.8 Hz, 2H), 8.51 (t, *J* = 1.8 Hz, 2H), 7.72 (dd, *J* = 3.2 Hz, *J* = 6.7 Hz, 4H), 7.45 (t, *J* = 3.8 Hz, 2H), 7.40−7.44 (m, 8H), 7.34−7.37 (m, 4H), 7.27−7.29 (m, 8H), 7.11 (d, *J* = 9.4 Hz, 4H), 6.95 (dd, *J* = 3.5 Hz, *J* = 5.9 Hz, 2H), 6.87 (dd, *J* = 3.2 Hz, *J* = 5.6 Hz, 4H), 6.70 (dd, *J* = 3.2 Hz, *J* = 5.8 Hz, 2H), 6.58 (dd, *J* = 2.9 Hz, *J* = 7.0 Hz, 4H), 6.30 (d, *J* = 9.1 Hz, 4H), 5.88 (dd, *J* = 2.9 Hz, *J* = 5.9 Hz, 4H), 5.34 (d, *J* = 3.8 Hz, 4H), 4.83 (s, 8H), 4.74 (d, *J* = 3.7 Hz, 4H), 1.50 (s, 18H); ^{13}C NMR (150 MHz, $CDCl_3$) δ 183.6, 180.8, 168.9, 167.8, 154.5, 152.6, 149.5, 143.0, 136.2, 134.9, 133.9, 133.6, 130.8, 130.2, 129.8, 129.5, 128.7, 128.5, 128.0, 126.8, 126.7, 125.9, 124.5, 124.2, 123.1, 121.9, 119.7, 118.6, 114.1, 112.9, 55.2, 51.7, 35.5, 31.6; HRMS (ESI-TOF) calcd for $C_{106}H_{93}N_6O_6$ [M + H] 1545.7151, found 1545.7121; λ_{max} abs 655 nm; λ_{max} em 696 nm.

*Data for squaraine rotaxane **18**:* ^{1}H NMR (600 MHz, $CDCl_3$) δ 10.1 (t, *J* = 1.7 Hz, 2H), 8.55 (d, *J* = 1.4 Hz, 4H), 7.68 (t, *J* = 4.1 Hz, 4H), 7.35−7.39 (m, 8H), 7.29−7.34 (m, 4H), 7.18 (d, *J* = 9.1 Hz, 4H), 6.83 (dd, *J* = 3.2 Hz, *J* = 5.6 Hz, 8H), 6.74 (dd, *J* = 2.9 Hz, *J* = 5.3 Hz, 4H), 6.54 (dd, *J* = 2.9 Hz, *J* = 5.6 Hz, 4H), 6.18 (d, *J* = 9.4 Hz, 4H), 5.95 (dd, *J* = 2.9 Hz, *J* = 5.9 Hz, 8H), 4.79 (s, 8H), 4.72 (d, *J* = 4.1 Hz, 8H), 1.48 (s, 18H); HRMS (ESI-TOF) calcd for $C_{112}H_{96}N_6O_6Na$ [M + Na] 1643.7284, found 1643.7287; λ_{max} abs 652 nm; λ_{max} em 700 nm.

*N-Phenylazepane (**20**).* Iodobenzene (1.64 g, 8.04 mmol) and hexamethyleneimine (0.875 g, 8.83 mmol) were combined in a dry round-bottom flask containing dimethylethanolamine (13 mL), CuI (210 mg, 1.10 mmol), and K_3PO_4 (4.49 g, 21.2 mmol). The mixture was heated at 100 °C for 20 h under an atmosphere of argon, at which point the reaction was quenched with water (150 mL) and the product extracted with ether (3 × 50 mL). The ether was dried over $MgSO_4$ and evaporated under reduced pressure to yield a crude material that was purified by silica gel column chromatography. A 30:70 (v/v) chloroform/hexanes eluent was used to obtain pure **20** (3.4% yield, 48.8 mg, 0.278 mmol) as a clear viscous oil: ^{1}H NMR (500 MHz, $CDCl_3$) δ 7.22−7.27 (m, 2H), 6.71−6.75 (m, 2H), 6.67 (tt, *J* = 1.0 Hz, *J* = 7.2 Hz, 1H), 3.47−3.51 (m, 4H), 1.79−1.85 (m, 4H), 1.58 (quint, *J* = 2.6 Hz, 4H); ^{13}C NMR (125 MHz, $CDCl_3$) δ 149.1, 129.4, 115.3, 111.3, 49.2, 28.0, 27.4.

*N-Methyl-N-(2-(prop-2-yn-1-yloxy)ethyl)aniline (**21**).* A NaOH (aq) solution was prepared by dissolving NaOH (18 g) in H_2O (30 mL). Reactant 2-(methylphenylamino)ethanol (3.0 mL, 31 mmol) was dissolved in toluene (40 mL) and slowly added over the basic aqueous layer. Phase-transfer catalyst tetrabutylammonium bisulfate (90 mg, 0.12 mmol) and propargyl bromide (18 mL, 200 mmol) were added to the toluene layer, and the reaction was gently stirred for 18 h. The organic layer was isolated, dried over $MgSO_4$, and evaporated under reduced pressure, affording **21** as a light brown oil (73% yield, 4.27 g, 22.7 mmol) that was used without further purification: ^{1}H NMR (500 MHz, $CDCl_3$) δ 7.30−7.34 (m, 2H), 6.78−6.83 (m, 3H), 4.22 (d, *J* = 2.4 Hz, 2H), 3.77 (t, *J* = 6.1 Hz, 2H), 3.63 (d, *J* = 6.1 Hz, 2H), 3.06 (s, 3H), 2.50 (t, *J* = 2.4 Hz, 1H); ^{13}C NMR (125 MHz, $CDCl_3$) δ 149.2, 129.3, 116.5, 112.3, 79.8, 74.7, 67.5, 58.5, 52.4, 39.0; HRMS (ESI-TOF) calcd for $C_{12}H_{16}NO$ [M + H] 190.1226, found 190.1215.

*N-Methyl-N-(undec-10-yn-1-yl)aniline (**22**).* A mixture of 11-bromo-1-undecyne (567 mg, 2.61 mmol), *N*-methylaniline (384 mg, 3.58 mmol), and potassium carbonate (4.10 g, 28.9 mmol) in acetonitrile was refluxed for 18 h. The resulting mixture was cooled to room temperature and filtered over Celite. The filtrate was collected, dried over $MgSO_4$, and evaporated under reduced pressure to yield crude material that was purified by silica gel column chromatography. A 50:50 (v/v) chloroform/hexanes eluent was used to obtain pure **22** (38% yield, 253 mg, 0.982 mmol) as a clear, viscous oil: ^{1}H NMR (600 MHz, $CDCl_3$) δ 7.29−7.33 (m, 2H), 7.75−7.79 (m, 3H), 3.38 (t, *J* = 7.7 Hz, 2H), 3.00 (s, 3H), 2.27 (td, *J* = 2.6 Hz, *J* = 7.0 Hz, 2H), 2.02 (t, *J* = 2.6 Hz, 2H), 1.66 (pent, *J* = 7.6 Hz, 2H), 1.61 (pent, *J* = 7.6 Hz, 2H), 1.46−1.51 (m, 2H), 1.37−1.42 (m, 8H); ^{13}C NMR (150 MHz, $CDCl_3$) δ 149.4, 129.2, 115.9, 112.2, 84.8, 68.3, 52.9, 38.4, 29.6, 29.2, 28.8, 28.6, 27.3, 26.8, 18.5; HRMS (ESI-TOF) calcd for $C_{18}H_{28}N$ [M + H] 258.2216, found 258.2205.

Computational Methodology. Density functional theory (DFT) calculations were performed using Gaussian 09 (see the Supporting Information for the complete reference). All structures were optimized without constraints at the M06/6-31G* level of theory. Thermal corrections were calculated at the same level of theory. All calculations used a polarizable continuum model (PCM) with parameters for chloroform to account for solvation effects. This level of theory generally allowed calculations of our SREP model to optimize within 2 days, a practically acceptable duration. Single-point energies of the optimized structures were calculated at the M06/6-311+G** level of theory with the PCM model for chloroform and added to thermal corrections to obtain free energy values. The crystal structure of monoendoperoxide macrocycle **1EP** and a previously published crystal structure of rotaxane **16** were modified to provide the starting structures for the DFT optimizations.[5] Optimized structures for the lowest energy conformations and background calculations are provided in the Supporting Information.

Determination of SREP-int Stereoisomer Stability. The rate of decomposition of **SREP-int** was monitored with ^{1}H NMR spectroscopy. A sealed sample of **5EP-int** in $CDCl_3$ was stored in the dark at 38 °C, and decomposition was monitored over 30 days. The sample was doped with anisole, which was used as an internal standard. Anisole is a stable, high boiling compound (bp = 154 °C), and therefore, we assumed no internal standard was lost through evaporation or decomposition. Decomposition kinetics were determined by integrating the bridging isophthalamide proton *C* of the surrounding macrocycle relative to the anisole methyl signal. The **5EP-int** half-life was ∼350 h.

■ ASSOCIATED CONTENT

Supporting Information

Spectral data, kinetic studies, X-ray structure details, and expanded computational results. This material is available free of charge via the Internet at http://pubs.acs.org.

■ AUTHOR INFORMATION

Corresponding Author

*E-mail: smith.115@nd.edu.

Notes

The authors declare no competing financial interest.

■ ACKNOWLEDGMENTS

This work was supported by the University of Notre Dame and the NSF. We thank Dr. Per-Ola Norrby and the anonymous peer reviewers of this article for their valuable comments.

■ REFERENCES

(1) Baumes, J. M.; Gassensmith, J. J.; Giblin, J.; Lee, J. J.; White, A. G.; Culligan, W. J.; Leevy, W. M.; Kuno, M.; Smith, B. D. *Nature Chem.* **2010**, *2*, 1025.

(2) Collins, C. G.; Baumes, J. M.; Smith, B. D. *Chem. Commun.* **2011**, *47*, 12352.

(3) Lee, J. J.; Goncalves, A.; Smith, B.; Palumbo, R.; White, A. G.; Smith, B. D. *Aust. J. Chem.* **2011**, *64*, 604.
(4) Lee, J. J.; White, A. G.; Rice, D. R.; Smith, B. D. *Chem. Commun.* **2013**, *49*, 3016.
(5) Baumes, J. M.; Murgu, I.; Oliver, A.; Smith, B. D. *Org. Lett.* **2010**, *12*, 4980.
(6) Baumes, J. M.; Murgu, I.; Connell, R. D.; Culligan, W. J.; Oliver, A. G.; Smith, B. D. *Supramol. Chem.* **2012**, *24*, 14.
(7) For further discussion of the mechanism of self-illumination and the hypothesis that the rate of SREP cycloreversion controls the chemiluminescence emission intensity, see: Smith, B. D. *Proc. SPIE* **2011**, 791013.
(8) For a systematic summary of rotaxane isomerism, see: Yerin, A.; Wilks, E. S.; Moss, G. P.; Harada, A. *Pure Appl. Chem.* **2008**, *80*, 2041.
(9) Gassensmith, J. J.; Baumes, J. M.; Eberhard, J.; Smith, B. D. *Chem. Commun.* **2009**, 2517.
(10) Typically, the role of a molecular template in a templated synthesis is to promote a specific reaction pathway, but in this case, the purpose of the encapsulated squaraine template is to prevent an undesired cycloaddition reaction of singlet oxygen with the second anthracene unit in macrocycle **1**.
(11) Collins, C. G.; Peck, E. M.; Kramer, P. J.; Smith, B. D. *Chem. Sci.* **2013**, *4*, 2557.
(12) If the encapsulated squaraine template has smaller end groups, the SREP is susceptible to transient dethreading in chloroform solution and undesired cycloaddition of another molecule of singlet oxygen to the free macrocycle **1EP**.
(13) Aubry, J. M.; Pierlot, C.; Rigaudy, J.; Schmidt, R. *Acc. Chem. Res.* **2003**, *36*, 668.
(14) Gassensmith, J. J.; Arunkumar, E.; Barr, L.; Baumes, J. M.; DiVittorio, K. M.; Johnson, J. R.; Noll, B. C.; Smith, B. D. *J. Am. Chem. Soc.* **2007**, *129*, 15054.
(15) While squaraines **12** and **13** cannot enter the cavity of macrocycle monoendoperoxide **1EP**, they readily associate inside the more spacious macrocycle **1**.
(16) High sensitivity of pseudorotaxane threading/unthreading to the size of the squaraine end groups has been observed in a related system with a different macrocycle. X-ray crystal structures suggest that a squaraine *N*-methyl group is constrained to remain within the squaraine aromatic conjugation plane, whereas the terminal methyl of an *N*-ethyl group protrudes out of the plane and creates significant steric bulk Lai, C. C.; Liu, Y. H.; Wang, Y.; Peng, S. M.; Chiu, S. H. *Org. Lett.* **2007**, *9*, 4523. Hsueh, S. Y.; Lai, C. C.; Liu, Y. H.; Peng, S. M.; Chiu, S. H. *Angew. Chem., Int. Ed.* **2007**, *46*, 2013.
(17) It is worth noting that the same rate of cycloreversion was obtained when rotaxane **15-ext** was dissolved in acetone. In other words, there was no evidence that the more polar solvent allowed the oxidized macrocycle to alleviate mechanical bond strain by translocating away from the central squaraine station to a sterically less demanding location over one of the rotaxane's two long alkyl chains. Additional experiments using even more polar solvents such as DMSO or DMF were not possible due to nucleophilic attack of the exposed squaraine by the solvent.
(18) Klanderman, B. H.; Criswell, T. R. *J. Org. Chem.* **1969**, *34*, 3426.
(19) Masci, B.; Pasquale, S.; Thuery, P. *Org. Lett.* **2008**, *10*, 4835.
(20) Xue, M.; Su, Y. S.; Chen, C. F. *Chem.—Eur. J.* **2010**, *16*, 8537.
(21) Luo, S. L.; Zhang, E. L.; Su, Y. P.; Cheng, T. M.; Shi, C. M. *Biomaterials* **2011**, *32*, 7127.
(22) Hilderbrand, S. A.; Weissleder, R. *Curr. Opin. Chem. Biol.* **2010**, *14*, 71.
(23) Arun, K. T.; Ramaiah, D. *J. Phys. Chem. A* **2005**, *109*, 5571.
(24) For discussions of conventional intramolecular steric effects on addition and release of oxygen to aromatic compounds, see: (a) Fudickar, W.; Linker, T. *Chem.—Eur. J.* **2006**, *12*, 9276. (b) Wasserman, H. H.; Wiberg, K. B.; Larsen, D. L.; Parr, J. *J. Org. Chem.* **2005**, *70*, 105. (c) Schmidt, R.; Brauer, H.-D. *J. Photochem.* **1986**, *34*, 1. (d) Lapouyade, R.; Desvergne, J. P.; Bouas-Laurent, H. *Bull. Soc. Chim. Fr.* **1975**, *9*, 2137. (e) Castillo, A.; Greer, A. *Struct. Chem.* **2009**, *20*, 399.
(25) In response to a reviewer request, we calculated how the energy of free 9,10-dimethylantharacene-9,10-endoperoxide changes with dihedral angle. The results of the calculations are shown in Figure S24 (Supporting Information) and indicate a quadratic dependency.
(26) For a recent mechanistic study of singlet oxygen cycloaddition to anthracene, see: Klaper, M.; Linker, T. *Angew. Chem., Int. Ed.* **2013**, *52*, 11896.
(27) For examples of steric control of singlet oxygen cycloaddition in synthetic organic chemistry, see: (a) Adam, W.; Bosio, S. G.; Turro, N. J. *J. Am. Chem. Soc.* **2002**, *124*, 8814. (b) Adam, W.; Guthlein, M.; Peters, E. M.; Peters, K.; Wirth, T. *J. Am. Chem. Soc.* **1998**, *120*, 4091.
(28) Zehm, D.; Fudickar, W.; Linker, T. *Angew. Chem., Int. Ed.* **2007**, *46*, 7689.
(29) Leigh, D. A.; Lusby, P. J.; Slawin, A. M.; Walker, D. B. *Angew. Chem., Int. Ed.* **2005**, *44*, 4557.
(30) For discussions of strain energy in enzymology, see: (a) Bugg, T. D. H. *Wiley Encyclopedia of Chemical Biology*; Begley, T. P., Ed.; Wiley: Hoboken, 2009; Vol. *1*, p 653. (b) Hayashi, H.; Mizuguchi, H.; Miyahara, I.; Islam, M. M.; Ikushiro, H.; Nakajima, Y.; Hirotsu, K.; Kagamiyama, H. *Biochim. Biophys. Acta* **2003**, *1647*, 103. For examples of small molecule strain and reactivity changes upon binding, see: (c) Kraka, E.; Tuttle, T.; Cremer, D. *Chem.—Eur. J.* **2007**, *13*, 9256. (d) Bahr, N.; Güller, R.; Reymond, J.-L.; Lerner, R. A. *J. Am. Chem. Soc.* **1996**, *118*, 3550.
(31) Farnum, D. G.; Webster, B.; Wolf, A. D. *Tetrahedron Lett.* **1968**, 5003.
(32) Fang, Y.; Zheng, Y. Q.; Wang, Z. Y. *Eur. J. Org. Chem.* **2012**, 1495.